rf susceptibility of single-crystal $CrBr_3$ near the Curie temperature

V. A. Alyoshin, V. A. Berezin, and V. A. Tulin
Institute of Microelectronics Technology, Russian Academy of Sciences, Chernogolovka, Moscow Region, 142432, Russia
(Received 16 October 1996; revised manuscript received 6 March 1997)

The high-frequency susceptibility of the ferromagnet $CrBr_3$ near the Curie temperature is investigated both in the ferromagnetic and paramagnetic states. The temperature dependences of the (1) intensity and linewidth of electron spin resonance (ESR), (2) effective field of the magnetic anisotropy, and (3) behavior of an imaginary part of the magnetic susceptibility in the region of homogeneous magnetization of a sample are obtained. The approximation of the ESR line intensity dependence on temperature gives $I \sim 1/(T-T_0)^{\gamma}$, where $\gamma = 1.307$ and $T_0 = 32.1$ K. The behavior of the ESR linewidth above the critical temperature is well described as $\delta H \sim 1/(T-T_0)^{\nu}$, $\nu = 0.5 \pm 0.05$). Determination of the transition point from characteristic features of ferromagnetic and paramagnetic states gives the transition temperature $T_C = 33$ K. The effective field of the magnetic anisotropy is $H_A(T) = H_A(0)(1-T/T_c)^{1/2}$. An imaginary component of the parallel susceptibility in a homogeneously magnetized state demonstrates the dependence: $\chi'' \approx \exp[(H_0-H)/a(T-T_1)]$, where $a = 197.2$ Oe/K, $H_0 = 1380$ Oe, and $T_1 = 29.8 \pm 0.2$ K. The same temperature corresponds to the maximum of absorption in a zero magnetic field. Assuming that the critical temperature is the temperature of susceptibility maximum in a zero magnetic field (29.8 K), the temperature dependence $I(T)$ has an index $\gamma \approx 2$, whereas the dependence of the ESR linewidth on temperature has the index $\nu \approx 0.8$. [S0163-1829(97)07125-7]

INTRODUCTION

Critical phenomena near the temperature of paramagnetic-ferromagnetic transition have been the subject of extensive studies for many years. On the one hand, these phenomena are subject to the general phase transition theory of second order,[1] which is characterized by a peculiar behavior of an order parameter. For ferromagnets, this parameter is the modulus of spontaneous magnetization. On the other hand, investigations of these critical phenomena could provide both better insight into details of the ferromagnetic system behavior and support for one of the existing models of magnetic ordering. The known ferromagnets are mainly metallic substances (metals, alloys, and intermetallic compounds). However, a few ferromagnetic insulators are known. Representing an example of the three-dimensional (3D) Heisenberg system, ferromagnetic insulators are simpler for theoretical investigations, which makes them preferable for experimental studies. There are many theoretical papers (see Ref. 2 and references therein) and very few experimental works on such 3D ferromagnetic insulators, which primarily deal with Eu-containing compounds like EuO and EuS.[3,4]

$CrBr_3$ is one of the ferromagnetic insulators. It was investigated by Tsubokawa[5] in 1960. The magnetic system of $CrBr_3$ is a good example of the Heisenberg ferromagnet. Unlike cubic EuO and EuS, it has a hexagonal crystalline structure of the BiI_3 type. Below 32.5 K,[6] $CrBr_3$ is a ferromagnet having anisotropy of an easy-axis type (the sixthfold axis of a crystal). The magnitude of the effective field of magnetocrystalline anisotropy was estimated by Dillon,[7] on the basis of the data from a ferromagnetic resonance investigation ($H_A = 6.8$ kOe). The neutron studies[8] showed that the exchange interaction is described by five constants. In simplified computations, describing experimental results satisfactorily, the exchange interaction can be described by two constants, one of which is in the hexagonal layer and the other is in the interlayer plane.[9] The dependence of magnetization on temperature and magnetic field was investigated in a number of works by the nuclear magnetic resonance (NMR) technique.[9–13] The measurements were made in the temperature range below 20 K, where a NMR signal can be observed. The results obtained were described using spin-wave theory and its expansion, which takes higher orders of interaction into account.

Data on the $CrBr_3$ behavior near the critical temperature are also available in the literature. In his book,[6] Kittel presents the data on the critical behavior of the susceptibility above T_C ($\gamma = 1.215 \pm 0.02$) and magnetization below T_C ($\beta = 0.368 \pm 0.005$), unfortunately, without referring to the original work. The data on the measurements of the electronic spin resonance linewidth in $CrBr_3$ above the critical temperature are reported in the book by White[14] where the dependence $(T-T_C)^{0.25}$ is described as due to the exchange narrowing. Thus the temperature dependence and critical behavior of this substance have been investigated fairly well.

We studied the rf-susceptibility dependence on temperature and magnetic field of $CrBr_3$ single crystals in the temperature range including the critical temperature, considering the sample to be a 3D Heisenberg ferromagnet. This work reports the results obtained and their discussion.

EXPERIMENTAL DETAILS

Single crystals of $CrBr_3$, grown by the gas transport technique,[15] were thin plates less than 50 μm thick, with lateral sizes of about 1 cm. For experimental study, 3 $\times$5 mm rectangles were cut out so that the axis of easy magnetization (c_6 axis) was perpendicular to the plate plane.

The experimental setup was arranged on the power-through spectrometer principle. A rf signal from the generator of sweeping frequency (central frequency in the range 100–1000 MHz) was supplied to the absorbing cell

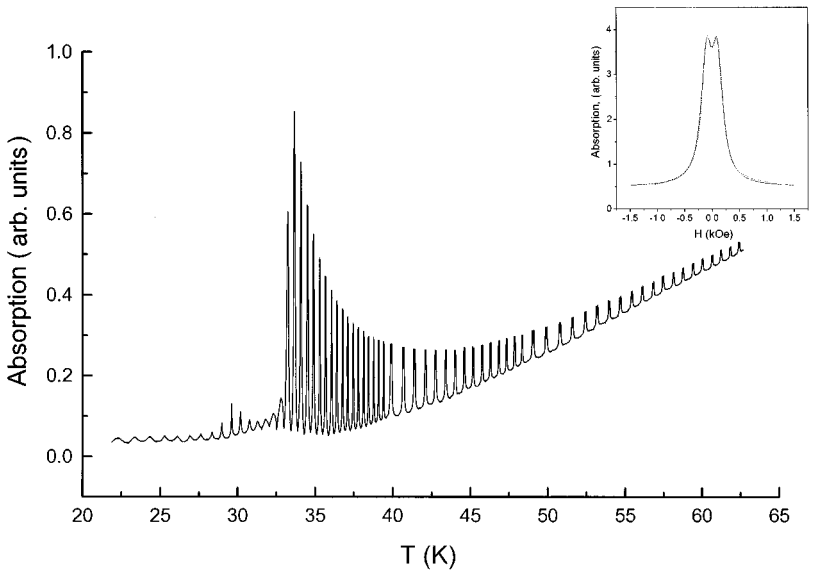

FIG. 1. Temperature dependence of the rf absorption ($f=363$ MHz) of $CrBr_3$ in sweeping from -1050 to $+1050$ Oe external magnetic field [type (b) of the electromagnet operation]. The external magnetic field is parallel to the c_6 axis of the sample and perpendicular to the rf magnetic field. The dependence of rf absorption on the external magnetic field at $T=38.9$ K in the same configuration is shown in the inset (dots are experimental data: solid line is the result of approximation).

through the coaxial line. The absorbing cell was a helix with a sample inside which was placed so that the rf magnetic field was parallel both to the plate plane and helix axis. The helix was made of a copper wire 0.2 mm in diameter; the diameter of the helix was 4 mm. A sample was placed between the insulating plates. The helix was inserted into a copper tube (30 mm long and 10 mm in diameter) using a dielectric holder. Two coaxial conductors, fastened to the tube, were made of thin-walled stainless-steel tubes. They were the holder of the whole construction, through which high-frequency power was brought to and removed from the absorbing cell. Communication with the helix was effected by the capacitive technique, that is, by placing the central conductors of the coaxials at the ends of the helix without any electrical contact. An amplitude of frequency modulation of the rf generator was about the resonator passband. In the low-frequency range (160–360 MHz), a LC circuit was used as an absorbing cell.

A signal, passed through the resonator, was supplied through the second coaxial line to the preliminary amplifier and detector in succession. Then the signal was brought to the peak detector and, if necessary, to the differential amplifier. A detected and amplified signal was supplied to a computer. The amplitude-frequency characteristic of the resonator during measurements was observed on the oscilloscope screen. The helix was located inside a helium cryostat. The cryostat jacket was filled with liquid nitrogen. To reach temperatures in the range 4.2–77 K, a small amount of liquid helium was poured into the cryostat. A heating element was placed inside the cryostat, on an additional metal screen, which allowed us to vary temperature in the range of interest. The cryostat was positioned between the poles of an electromagnet which could be rotated around its vertical axis. The helix and sample were arranged so that the helix axis was horizontal and the sample plane vertical and parallel to the axis. By turning the magnet, the following orientations of the uniform external field **H** could be achieved: (1) parallel to the helix axis and, therefore, perpendicular to the c_6 axis of a sample and (2) perpendicular to the helix axis and parallel to the easy magnetization axis. Orientations were set by checking the sample response. Two different ways of varying the externally applied magnetic field were used in our work: (a) The magnitude of the external magnetic field was increased (decreased) from 0 to 7 kOe at a certain rate and (b) the magnetic field was varied in a sawtooth manner with time, with the field uniformly increasing from -1050 to $+1050$ Oe and then returning to -1050 Oe and so on. Field intensity was measured by a Hall gauge. Temperature was determined by measuring the resistance of a carbon thermometer, placed on the copper tube. The readings of both the Hall gauge and the thermometer were also read out on a computer.

Changes in the rf power, passed through the resonator with a sample, were registered. At a constant power supplied to the resonator, the changes were proportional to the change of an imaginary part of the high-frequency susceptibility of a sample, provided the resonator parameters were independent of magnetic field and temperature.

EXPERIMENTAL RESULTS

Changes in the characteristic properties of rf-field absorption by a sample depending on the external magnetic field H were studied in the temperature range 20–65 K. The resonant frequency of the LC circuit at $T=4.2$ K was 363 MHz. As liquid helium evaporated, the temperature slowly increased to 65 K within approximately 1 h. The external magnetic field H was parallel to the easy magnetization axis and, at the same time, perpendicular to the rf magnetic field. It was varied according to procedure (b) with the frequency of oscillations equal to 2×10^{-2} Hz. That is, as the temperature increased from 20 to 65 K, approximately 60 cycles of magnetic field variation were performed in a continuous manner.

Figure 1 presents the curve obtained in the experiment. It can be arbitrarily divided into three parts. At temperatures below $T=28.8$ K (T is the absolute temperature), the dependence of the absorption on the magnitude of the external magnetic field H is the following: The absorption maxima correspond to the zero-field value and the minima to its maximum value (by amplitude). As the temperature grows, a sharp increase in the absorption in the zero field is observed, reaching a maximum at $T=29.8$ K. At $T=33$ K, the field

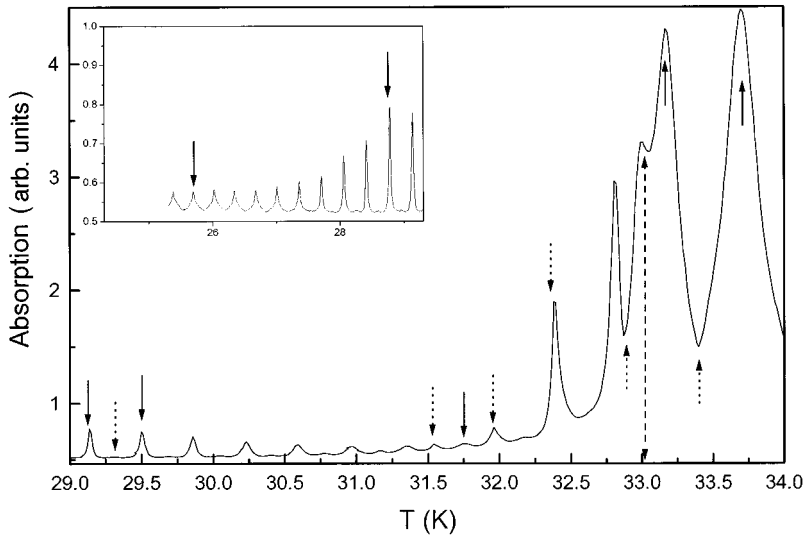

FIG. 2. Temperature dependence of the rf absorption ($f=600$ MHz) by $CrBr_3$ in sweeping from -1050 to $+1050$ Oe external magnetic field. The external magnetic field is perpendicular to the c_6 axis of the sample and parallel to the rf magnetic field. The solid arrows mark the maxima which correspond to the zero value of a sweeping field, and the dotted arrows mark the maxima which correspond to the maximum (by amplitude) value of a sweeping field. The dotted arrow marks the phase transition.

dependence of the signal changes again. The lines of intense absorption, arising at this temperature, correspond to electron spin resonance (ESR). Evidently, the sample is paramagnetic above this temperature. Each line consists of two ESR lines, corresponding to the value of resonant field $H_{\rm res}=\pm\omega_{\rm res}/\gamma^*$ (γ^* gyromagnetic ratio of Cr^{3+} ion). Until the line half-width is greater than the value of the resonant field, the maximum of absorption is in the zero field. As the temperature grows, the half-width decreases and the absorption dependence on the magnetic field is described by the curve presented in the inset of Fig. 1. Moreover, a total growth of absorption at temperatures above 30 K is seen in Fig. 1, apparently caused by an increase in the specific resistance of copper, which is the basic element of the absorbing cell.

Similar measurements were made using another experimental configuration. The external magnetic field was applied parallel both to the surface of the sample and to the rf field, and was oscillated at an amplitude from -1050 to $+1050$ Oe [type (b)]. The resonant frequency of the helix at $T=4.2$ K was 600 MHz. The temperature was varied in the range 24–45 K. The technique of the experiment was similar to that described above. The experimental curve is shown in Fig. 2.

In the same configuration, the rf-absorption dependence on magnetic field H was studied at a fixed temperature [type (a) of electromagnet operation]. The external field was increased from 0 to 6 kOe. The temperature of each measurement was maintained constant. Some selected curves are shown in Fig. 3.

Up to a temperature below 29 K in Fig. 2, the maxima of absorption correspond to a zero value of the magnetic field H. These maxima are marked by solid arrows. At 29 K, an abrupt increase in the absorption in the zero field occurs (this increase is also seen in one of the curves in Fig. 3 as a sharp peak at $H=0$). Above 29 K, additional maxima begin to appear between the earlier marked ones. They are marked by pointed arrows and correspond to the maximum (by amplitude) value of an oscillating magnetic field. In Fig. 3, all the curves exhibit a peak of absorption. At low temperatures, this peak is observed in the region of rather large fields. The peak is due to the resonance of domain wall displacement in the region of the domain structure instability, disappearing as it approaches the saturation field of magnetization of a sample, H_S.[16] With an increase in the temperature, it shifts towards smaller fields and at about 29 K it appears in the region of field oscillation (Fig. 3). Upon further growth of

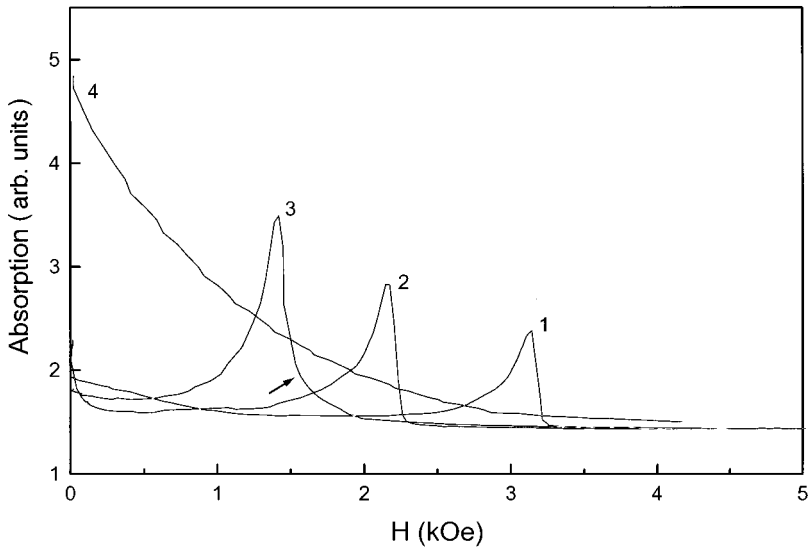

FIG. 3. Dependence of the rf-field absorption in $CrBr_3$ on the external magnetic field [type (a) of the electromagnet operation]. The external magnetic field is perpendicular to the c_6 axis and parallel to the rf magnetic field. Curve 1 corresponds to the temperature 24.1, 2–28.8, 3–31, and 4–35.4 K. The arrow at curve 3 marks the transition of a sample into a homogeneously magnetized state.

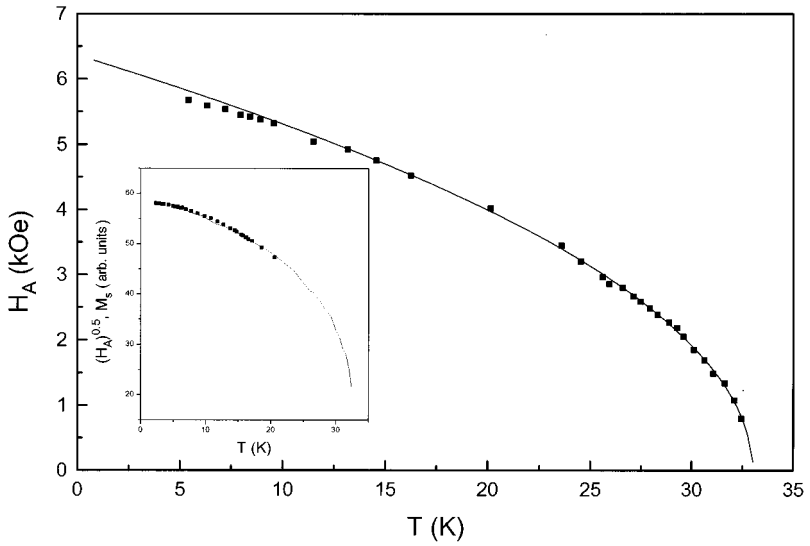

FIG. 4. Dependence of the anisotropy field H_A on temperature (dots are the experimental data; (solid line is the result of approximation). In the inset, the saturation magnetization $M_S(T)$ is shown by dots and $(H_A)^{0.5}(T)$ by a solid line.

the temperature, a larger part of the peak appears within the 1 kOe limits, which is accompanied by the growth of the amplitude of additional maxima in Fig. 2. The sharp maximum at 32.8 K corresponds to the situation when the whole peak was registered. At $T_C=33$ K, the feature of absorption is seen in Fig. 2, marked by the dotted arrow. At this temperature, the sample passes into the paramagnetic state, and the maximum of absorption corresponds to the trace of spin resonance in the zero magnetic field and further suppression of the resonance absorption by a magnetic field when the dc magnetic field is parallel to the orientation of the rf magnetic field. That is, within one cycle of the field oscillation the sample was first ferromagnetic (and we observed the maximum of absorption, corresponding to the transition of the substance into a homogeneously magnetized state) and then became paramagnetic (and we observed a trace of paramagnetic resonance).

If the amplitude of an external magnetic field, applied perpendicular to the anisotropy axis (i.e., parallel to the sample surface), is increased, then at some magnitude of the field the sample will pass into a homogeneously magnetized state. This field, referred to as a saturation field, is equal to $H_S=H_A+4\pi N_\perp M_S$,[9] where H_A is the field of anisotropy, M_S is the saturation magnetization, and $N_\perp$ is the demagnetizing factor in the direction perpendicular to the anisotropy axis. In Fig. 3, the value of this field is marked by an arrow. We defined it as the upper (by field) boundary of absorption, with the resonance of domain wall displacement near the field of saturation magnetization. The position of this branch of the resonance with respect to the magnetic field is virtually independent of a frequency in the frequency range below 600 MHz for the sizes of samples used.[16] Because in this case the geometrical sizes of the sample are such that the demagnetizing factor in the c-axis direction is much higher than in any other direction perpendicular to it and the sum of the demagnetizing factors in three mutually perpendicular directions is equal to 1, we can consider that $N<0.05$ and $H_S(T)\approx H_A(T)$. The constructed temperature dependence of the anisotropy field is presented in Fig. 4. Although it slightly differs by its absolute value, this dependence does not contradict the results obtained by Dillon.[7]

PROCESSING AND DISCUSSION OF THE RESULTS

In order to determine the temperature dependence of the ESR line intensity, the following procedure was adopted. A change in absorption due to the specific resistance of copper was subtracted from the curve in Fig. 1. The curve in the region of the ESR appearance was divided into plots, limited by the points of a minimum level of absorption, to which the external magnetic field values, $H=\pm 1050$ Oe, correspond. Then each plot was renormalized to the range of magnetic field changes. As a result, a set of curves was obtained where each curve was the sum of two ESR lines corresponding to $H_{\rm res}=\pm\omega_{\rm res}/\gamma^*$. Assuming that an ESR line had the Lorentz form, each curve was fitted by the function

$$Y=a+b\left\{\frac{1}{(H-H_0)^2+d^2}+\frac{1}{(H+H_0)^2+d^2}\right\},$$

where H_0 is the resonant magnetic field and d is the line half-width. In the inset in Fig. 1, the dots represent one of these curves and the solid line is the result of approximation. This approximation allowed us to obtain the resonant magnetic field, width, and area of an ESR line.

The dependence of line half-width on temperature is presented in the inset of Fig. 5. The ordinate axis shows the logarithm of the half-width, and the abscissa axis shows the logarithm of the $T-T_0$ difference. Approximating the temperature dependence of the half-width near the Curie point by the function $d\sim 1/(T-T_0)^\nu$, we find $T_0=32.1$ K and $\nu=0.5\pm 0.05$. The result of this approximation is shown by the straight line 1 in the inset in Fig. 5. Along with the expected (due to fluctuations) growth of the half-width as the Curie point is approached, its reduction at high temperature is also observed, connected with the exchange narrowing, which is proportional to $(T-T_C)^{0.25}$.[14] In the inset in Fig. 5, this dependence is shown by straight line 2 in the high-temperature region.

Knowing b and d values, we can find the area of an ESR line at a given temperature and obtain the temperature dependence of the line intensity. This dependence is shown in Fig. 5. The ordinate axis shows the inverse intensity.

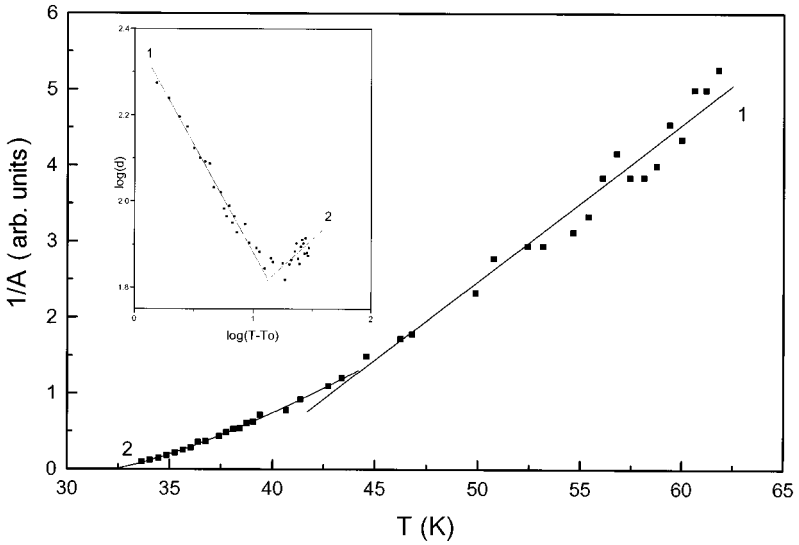

FIG. 5. Dependence of the inverse ESR line intensity on temperature. In the inset, the abscissa axis shows the logarithm of $(T-T_0)$ difference where $T_0=32.1$ K and the ordinate axis shows the logarithm of the ESR line half-width. Dots are the experimental data; solid line is the result of approximation.

Far from the Curie point, the dependence of absorption on temperature follows the law $1/(T-\theta)$ rather precisely, where θ has an appreciably higher value than the actual temperature of transition.[6] Approximating the part of the curve in Fig. 5 for temperatures above 44 K by this function, we obtain $\theta=38$ K. The result of the approximation is presented by curve 1. Near the temperature of the phase transition, the experimental results are described by the dependence $1/(T-T_0)^{\gamma}$, where $\gamma=1.307$ and $T_0=32.1$ K (curve 2).

A significant change of $\chi''(H)$ occurs in a field higher than the saturation one as seen in Fig. 3. This change increases as the transition temperature is approached. An attempt was made to approximate the parts of the curves. The exponent $\chi''=A(T)\exp[-H/b(T)]$ seems to be best suited for the purpose. From the set of the results obtained, $b(T)=a(T-T_1)$, where $T_1=29.8\pm0.2$ K. Then we considered the preexponential factor $A(T)$, which is represented in Fig. 6 (curve 1). It appeared that this factor also fits well the exponential dependence $B\exp[c/(T-T_1)]$ with the same value of T_1 where B and c are constants. Combining these dependences, we found that the set of these data is described by the expression $\chi''\sim\exp[(H_0-H)/b(T)]$. This approximation proved valid in the temperature range 31–35.4 K, where the magnitude of χ'' was measured. The approximation gave $H_0=1380$ Oe. The $b(T)$ dependence is represented by curve 2 in Fig. 6. It is well approximated by the function $b(T)=a(T-T_1)$, where $a=197.2$ Oe/K and $T_1=29.8\pm0.2$ K.

Let now consider the maximum of absorption in zero magnetic field at a temperature slightly below T_C (Figs. 2 and 3). It follows from the above reasoning that the $\chi''(T,H)$ behavior that the temperature of this maximum coincides with T_1. This fact is indicative of the interrelation between this maximum of absorption and the discussed above dependence $\chi''(T,H)$ at $T\rightarrow T_1$.

To explain these results, we turn to a well-known model of spontaneous magnetization occurrence in the framework of molecular field theory.[6] The model is connected with a graphic solution of the expression for magnetization in the form of a Brillouin function in which the argument involves a molecular field. An external magnetic field is usually neglected in the model. Taking an external magnetic field into account gives rise to a spontaneous magnetic moment at a temperature higher than the Curie temperature. Because the model does not include any mechanism to account for losses, we assume in our consideration that characteristic features of an imaginary component of the susceptibility are typical of features of its real component. According to the model, the real component also exhibits a characteristic feature at a tem-

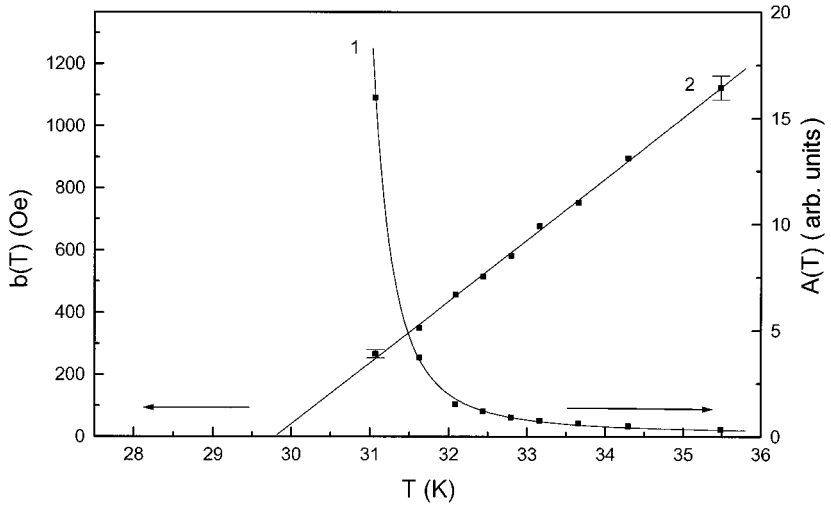

FIG. 6. Temperature dependences of approximative curve parameters A and b, describing the experimental behavior of an imaginary part of the parallel rf susceptibility $\chi''(T,H)=A(T)\exp[-H/b(T)]$.

perature equal to the Curie temperature. In our experiments, we measured the imaginary component of $\partial M/\partial H$ in a relatively strong magnetic field. The results show that its behavior is described by a relatively simple expression which exhibits a characteristic feature at a temperature much lower than that of the spontaneous moment occurrence ($T_1 = 29.8$ K, whereas $T_C = 33$ K). The spin-wave approach[17] is unsuitable in our case.

Processing of the data on an effective field of magnetic anisotropy near the Curie point (Fig. 4) takes the form

$$H_A(T) = H_A(0)(1 - T/T_C)^{1/2},$$

where $H_A(0) = 6.3$ kOe and $T_C = 33$ K is the transition temperature into a paramagnetic state. For a Cr^{3+} ion, the anisotropy has basically a dipole-dipole character. A comparison of the anisotropy field measured in the present work and the magnetization obtained from the NMR data[13] shows that the anisotropy field is proportional to the square magnetization in the temperature range 4.2–20 K (the inset in Fig. 4). We could measure a NMR signal in $CrBr_3$ only below 20 K. Assuming that this proportionality holds up to the Curie point, index β at $(T_C - T)$ in the magnetization dependence on temperature would be approximately equal to 0.25.

Now let us consider the mathematical processing of the experimental data. Because the set of data is limited, the computer processing of the dependences with three unknown parameters does not allow their precise determination. To avoid this, we tried to determine the characteristic temperatures from the experimental data, extrapolating them up to the intersection with the temperature axis. The obtained characteristic temperatures were substituted into the dependences, so that the computer should determine only indices and constants.

The presence of three characteristic values of temperature describing the phase transition of second order is an exceptional circumstance and needs some comment. Recall that the thickness of the sample is rather small (45 μm). This value primarily determines the domain structure parameters. When the space ranges of ferromagnetic fluctuations are higher or of the same order as the domain thickness and the characteristic times of fluctuations are much longer than the reversed frequency of the rf magnetic field, the domain structure can coexist with fluctuations and reveals itself during measurements. We measured the anisotropy field using the absorption signal, associated with the domain structure disappearance. Thus the temperature 33 K may be treated as the temperature at which the characteristic sizes of fluctuations may be in some relationship with the domains thickness. Treated in this way, the temperature 33 K would not be critical. Therefore the temperature of the absorption maximum in zero magnetic field, 29.8 K, can be substituted into the equation for the temperature dependence of the ESR line area as critical. An approximation of the experimental dependence of the ESR line area on temperature gives the index $\gamma \approx 2$. Thus the introduction of a single critical temperature removes one contradiction, but gives rise to another: a too high index of the temperature dependence of the ESR line area, which is inconsistent with scaling correlations.[1]

CONCLUSION

The high-frequency susceptibility of the ferromagnet $CrBr_3$ near the Curie temperature has been investigated both in the ferromagnetic and paramagnetic states. The following temperature dependences are determined: ESR intensity, ESR linewidth, effective field of magnetic anisotropy, and the behavior of an imaginary part of the magnetic susceptibility in the region of homogeneous magnetization of a sample. Three characteristic temperatures are observed. An approximation of the temperature dependence of ESR line intensity gives [$I \sim 1/(T - T_0)^{\gamma}$, where $\gamma = 1.307$], $T_0 = 32.1$ K. The same temperature value characterizes the ESR linewidth behavior above the critical temperature [$\delta H \sim 1/(T - T_0)^{\nu}$, $\nu = 0.5 \pm 0.05$]. Observation of the transition by characteristic features of ferromagnetic (domain wall absorption near the field of homogeneous magnetization) and paramagnetic (ESR) states gives the transition temperature $T_C = 33$ K. The same temperature is obtained from the approximation of an effective field of the magnetic anisotropy [$H_A(T) = H_A(0)(1 - T/T_C)^{1/2}$, where $H_A(0) = 6.3$ kOe is the anisotropy field at 0 K]. The result is to be expected, because the anisotropy field was evaluated from the absorption of domain walls. The lowest characteristic temperature is exhibited by an imaginary part of parallel susceptibility in the homogeneously magnetized state: $\chi'' \sim \exp[(H_0 - H)/a(T - T_1)]$, where $a = 197.2$ Oe/K, $H_0 = 1380$ Oe, and $T_1 = 29.8 \pm 0.2$ K. The same temperature corresponds to the maximum of absorption in zero magnetic field. The presence of these three various temperatures cannot be due to an inaccuracy of the experiment, because all these features can be obtained as the result of the processing of one measurement (Figs. 1 and 2). The temperature 33 K apparently corresponds to the coincidence of characteristic space ranges of fluctuations with domain structure dimensions, whereas the veritable transition temperature is that of the maximum of susceptibility in zero magnetic field (29.8 K). In this case the temperature dependence $I(T)$ has the index $\gamma \approx 2$ and the ESR linewidth dependence on temperature has the index $\nu \approx 0.8$.

ACKNOWLEDGMENT

The authors are grateful to Dr. V. I. Marchenko for his interest in this work and helpful discussions.

[1] L. D. Landau and E. M. Lifshitz, *Statistical Physics* (Nauka, Moscow, 1995), Pt. I, Chap. 14.

[2] D. P. Landau and Kun Chen, Phys. Rev. B **49**, 3266 (1994).

[3] L. Passell, O. W. Dietrich, and J. Als-Nielsen, Phys. Rev. B **14**, 4897 (1976).

[4] J. Als-Nielsen, O. W. Dietrich, and L. Passell, Phys. Rev. B **14**, 4908 (1976).

[5] I. J. Tsubokawa, J. Phys. Soc. Jpn. **15**, 1664 (1960).

[6] C. Kittel, *Introduction to Solid State Physics* (Wiley, New York, 1976), Chap. 16.

[7] J. F. Dillon, Jr., J. Appl. Phys. **33**, 1191 (1962).
[8] E. J. Samuelsen, R. Silberglitt, G. Shirane, and J. R. Remeika, Phys. Rev. B **3**, 157 (1971).
[9] C. H. Cobb, V. Jaccarino, M. A. Batler, J. P. Remeika, and H. Yasuoka, Phys. Rev. B **7**, 307 (1973).
[10] A. C. Gossard, V. Jaccarino, and J. P. Remeika, Phys. Rev. Lett. **7**, 122 (1961).
[11] A. C. Gossard, V. Jaccarino, and J. P. Remeika, J. Appl. Phys. **33**, 1187 (1962).
[12] C. H. Cobb, V. Jaccarino, J. P. Remeika, R. Silberglitt, and H. Yasuoka, Phys. Rev. B **3**, 1677 (1971).
[13] V. A. Tulin, M. Komu, E. Makela, P. Oksman, and M. Punkkinen, Pis'ma Zh. Eksp. Teor. Fiz. **35**, 462 (1982) [JETP Lett. **35**, 571 (1982)].
[14] R. M. White, *Quantum Theory of Magnetism* (McGraw-Hill, New York, 1970), Chap. 6.
[15] L. A. Klinkova and V. A. Bochkareva, Izv. Akad. Nauk SSSR, Neorg. Mater. **16**, 1777 (1980).
[16] V. A. Tulin, Pis'ma Zh. Eksp. Teor. Fiz. **31**, 585 (1980) [JETP Lett. **31**, 550 (1980)].
[17] H. L. Davis and A. Narath, Phys. Rev. **134**, 433 (1964).